Multichannel filtering for image texture segmentation

Trygve Randen (e-mail: tranden@hsr.no)
John Håkon Husøy (e-mail: jonh@hsr.no)

Rogaland University Center
Department of Electrical and Computer Engineering
P.O. Box 2557 Ullandhaug, N-4004 Stavanger, Norway
Phone: +47 51 87 40 00
Fax: +47 51 87 42 36

Abstract

Several approaches to multichannel filtering for texture classification and segmentation with Gabor filters have been proposed. The rationale presented for the use of the Gabor filters is their relation to models for the early vision of mammals as well as their joint optimum resolution in time and frequency. In this work we present a critical evaluation of the Gabor filters as opposed to filter banks used in image coding – in both full rate and critically sampled realizations. In the critically sampled case, tremendous computational savings can be realized. We further evaluate the commonly used octave band decomposition versus alternative decompositions.

We conclude that, for a texture segmentation task, several filters provide approximately the same results as the Gabor filter and, most important, it is possible to use sub-sampled filters with only a modest degradation in segmentation accuracy – realizing considerable computational savings.

Subject terms: Digital Image Processing, Pattern recognition, Texture segmentation, Texture classification, Perfect reconstruction filtering, Subband filtering, Multichannel filtering, Gabor filters.

1 Introduction

In several papers the successful application of multichannel filtering for texture segmentation is reported [1, 2, 3, 4, 5, 6, 7, 8, 9, 10]. Various filtering concepts have been applied, such as isotropic filters [10] and discrete cosine transform (DCT) [11], but the most popular channel filters utilized are the Gabor filters [12] designed to respond to different spatial frequency ranges. The rationale presented for the use of the Gabor filters is their relation to models for the early vision of mammals as well as their joint optimum resolution in time and frequency [12, 13]. A critical evaluation of the use of Gabor filters as opposed to alternative filter choices is not presented in the works referred to above.

In this paper, a broader point of view to the task of selecting filters for the filter banks is adopted. Rather than postulating a restricted class of filters such as the Gabor filters, we examine the performance of multichannel segmentation schemes based on more general classes of filters including the Gabor filters. It is shown that, for the present application, performances comparable to those obtained by the use of Gabor filters are obtained by other filters that can be implemented at a substantially lower computational cost.

It has been common to decompose the frequency band by the octave band (dyadic) decomposition [1, 2, 3, 5, 6, 7] (often referred to as the wavelet decomposition). This choice is motivated by the similarities between the octave band decomposition and the early vision of mammals. Octave band decomposition implies a finer frequency resolution in lower than in higher frequency regions. The work by Chang and Kuo [8], however, indicate that texture features are most prevalent in intermediate frequency bands. Thus, the octave band decomposition is not optimal. We present a broad range of subband decompositions, and thereby show that alternative decompositions are, in some cases, just as good as the octave band decomposition.

Most approaches to multichannel texture segmentation apply filter banks in which the subbands each *have the same number of image samples as the unfiltered image*. Thus, after filtering, the amount of data is increased by a factor corresponding to the number of frequency channels in the filter bank. It is well known that sub-sampling of the various frequency bands, in such a way that the total number of signal samples equals the number of signal samples in the input image, can be performed without losing any information as long as the filters are designed appropriately [14]. We examine what kind of segmentation can be obtained by operating on sub-sampled frequency channels when using critically sampled filter banks allowing perfect reconstruction of the input signal. By using this approach, tremendous computational savings can be realized.

The main results of our research are:

- Other filters than the Gabor class are useful in a texture segmentation context.

- Other subband decompositions than the octave band decomposition may also be suited for texture segmentation.

- By applying sub-sampled perfect reconstruction filter banks, good segmentation performance can be achieved at a significantly lower computational cost than what is the case for non-sub-sampled Gabor schemes.

2 Multichannel filtering for texture segmentation

Experiments done on cats and apes, which have a visual system similar to the human visual system [15], show that these animals decompose the visual images into several filtered images, with different spatial frequency ranges and tuned to different orientations [16]. This model is used for our texture segmentation scheme, and Figure 1 shows our general experimental setup. We will in the Fig. 1
following subsections describe the elements of this setup. We will go further into the details of the various filter banks in the Sections 3 and 4.

2.1 Local energy function

The objective of multichannel filtering, and the subsequent local energy function, is to transform the edges between the textures into detectable discontinuities [17]. The filter bank is in essence a set of bandpass filters with frequency and orientation selective properties and the local energy function is utilized for the purpose of transmitting areas in each channel where the band pass frequency components are strong into a high constant gray-level and areas where it is weak into a low constant gray-level.

We found the local energy function proposed by Farrokhnia [1, 2, 3] to be appropriate for our experiments. Thus we use

$$e_k = \left|\Psi\left(r_k(x,y)\right)\right|, \tag{1}$$

where

$$\Psi(t) = \tanh(\alpha t),$$

as the nonlinear transform, where $r_k(x, y)$ is the image corresponding to frequency channel no. k and (x, y) denote spatial coordinates. The parameter α gives the saturation characteristic of this function. By experience, $\alpha = 0.25$ [1, 2, 3].

The nonlinear transform is followed by a Gaussian low-pass (smoothing) filter of the form

$$H_G(u, v) = \frac{1}{\sqrt{2\pi}\sigma} e^{-\frac{1}{2\sigma^2}(u^2+v^2)}, \tag{2}$$

where

$$\sigma = \frac{\sqrt{2}}{2} \frac{1}{f_0}, \tag{3}$$

and f_0 is the radial center frequency from the band-pass filter. The center frequencies are normalized to the interval $[-1/2, 1/2]$. Gaussian filters have the property of giving accurate localization of the texture boundaries [1].

2.2 Classification

The output from the local energy function is a set of images, one image per filter in the filter bank. These images are the feature images, that will form the basis for the classification. We use these images to form feature vectors, where each feature image corresponds to one element in the feature vectors. Classification is the task of assigning these feature vectors to, hopefully, the right class.

We use the "Learning Vector Quantizing (LVQ)" supervised classifier of Kohonen [18, 19]. As is common in the work by Farrokhnia [1, 2, 3], we use a subset of 6% of the evaluation data-set as the training data-set. Tests verified that a subset of 6% is appropriate.

2.3 Test images

The choice of test images is not obvoius when we use sub-sampling. Texture mosaics like 'Nat-5', 'Nat-16' and most two-texture mosaics found in [1] have mainly straight vertical and horizontal texture edges. As can be seen from the experiments in Section 4, using a large sub-sampling rate results in a considerable blocking effect. When the block boundaries coincide with the texture boundaries, which is not likely to occur in real world images, the sub-sampled segmentation has an advantage over non-sub-sampled segmentation. Therefore we had to construct test images that had no vertical and horizontal edges. In our experiments we use the texture mosaics 'D17-D55', 'Nat-5b' and 'Nat-16b', see Figures 2, 3 and 4, all with natural textures from Brodatz [20]. Fig. 2

Fig. 3

Fig. 4

3 The Gabor filter approach

In this section we will review three different approaches to Gabor filtering for texture segmentation.

3.1 A fixed filter structure

Farrokhnia [1] proposes a bank of Gabor filters with even symmetry and an octave band decomposition. The decomposition is determined by the size of the input image, and is therefore fixed with respect to the characteristics of the textures in the input image. The frequency response of the Gabor filter is given by

$$H(u,v) = A \cdot e^{-\frac{1}{2}\left(\frac{(u-f_0)^2}{\sigma_u^2}+\frac{v^2}{\sigma_v^2}\right)} + A \cdot e^{-\frac{1}{2}\left(\frac{(u+f_0)^2}{\sigma_u^2}+\frac{v^2}{\sigma_v^2}\right)}, \tag{4}$$

where u and v are the vertical and horizontal frequencies, respectively, and f_0 is the radial center frequency of the actual channel. The f_0's are given by

$$\frac{1\sqrt{2}}{N_C}, \frac{2\sqrt{2}}{N_C}, \frac{4\sqrt{2}}{N_C}, \cdots \frac{\frac{1}{4}N_C\sqrt{2}}{N_C}, \tag{5}$$

where N_C is the input image width in number of pixels. For some textures, the lowest radial frequencies of Equation (5) are not very useful, because they capture features too corase to explain textural variations in an image [1]. Therefore, we only use the filters corresponding to the five highest radial frequencies in our texture segmentation – the same approach as Farrokhnia [1].

The parameters σ_u and σ_v, given by

$$\sigma_u = \frac{f_0}{3\sqrt{2\ln 2}} \tag{6}$$

$$\sigma_v = \frac{\tan 22.5^\circ f_0}{\sqrt{2\ln 2}}, \tag{7}$$

determine the widths of the pass-bands of the filters. Each filter is applied at four orientations, 0°, 45°, 90° and 135°.

As the segmentation quality measure we use the percentage of correctly classified pixels. The segmentation results for the Gabor filter are presented in Table 1 and the segmentation of the texture mosaics 'Nat-5b' and 'Nat-16b' are presented in Figures 5 and 6. Tab. 1 Fig. 5 Fig. 6

The method presented here gives good segmentation results, but a drawback with the method is its high computational complexity. With four orientations for each used radial center frequency in Equation (5) the resulting filter bank will have 20 filters for images 64×64 pixels and larger. All the feature images of an image like 'Nat-16b' of 512×512 pixels will therefore have a total of five million pixels! Farrokhnia [1, 2, 3] presents a way of reducing the number of feature images, but for the most complicated images this reduction leads to a not very good segmentation [1] – and even if the reduction is used, the computational complexity is still relatively high.

3.2 Optimal parameters

The method presented in the previous section applies a large set of filters, and has therefore a high computational complexity. If we can find *one* filter which leads to good segmentation, we will get large savings in computational complexity.

Dunn et.al. [17, 21, 22] suggests a method for finding the optimal Gabor filter for discriminating *two* textures. In this method, the resulting Gabor filter is a general Gabor filter, as opposed to the even-symmetric Gabor filter of the previous section.

We have applied this optimal Gabor filter design method in a multichannel filtering context. The method by Dunn et.al. [17, 21, 22] gives one filter per texture pair. For a multi-texture image, our filter bank then consists of the set of the optimal filters, one filter for each possible texture pair in the image.

Table 2 shows the experimental results. For 'D17-D55' we see a modest degradation from the previous method, but the computational savings are tremendous – by the previous method we had 20 feature images, now there's only one! For 'Nat-5b' the computational savings are less, ten filters versus 20, but here we have approximately no loss in the segmentation accuracy. Tab. 2

The method is, however, poor for some synthetic textures like 'S-IO', see Figure 7, which verifies the observation that a collection of filters gives better results than any single filter for textures of this kind [5]. For 'S-IO', this method had over 35% more misclassification than any of the other methods we tested. Other properties of this method are: Fig. 7

- The estimation of the optimal Gabor filter parameters is computationally demanding, so if it's impossible to perform this computation off-line, then much of the savings in computational complexity will be lost.

- In order to find the optimal parameters, we have to know the textures in advance, and therefore an unsupervised system is out of the question. In contrast, the previous method becomes unsupervised just by replacing the supervised classifier by an unsupervised classifier.

- The number of filters increases rapidly with the number of textures in an image, two textures implies one filter, five textures implies ten filters and n textures implies $(n-1)!$ filters. Consequently, the method is out of the question for 'Nat-16b' – it would have implied 15! filters.

In conclusion, this method may be an accurate and faster alternative to the previous method, if the circumstances are right, but for a large class of images and applications, the method is not suited.

3.3 Alternative subband decompositions

In Section 3.1 we used the octave band decomposition. The papers that suggest using the octave band decomposition usually give similarities with the human visual system as the argument for using this decomposition. In this section we will evaluate the octave band decomposition against some other decompositions, while still using the Gabor filter.

Some possible subband decompositions are given in Figure 8. In these experiments we have chosen to use the filter of Equation (4), the even symmetric Gabor filter. The center frequency, f_0, is set to the absolute value of the frequency in the center of the pass-band and the filter orientation is set to the corresponding angle. Fig. 8

The formulas for σ_u, Equation (6), and σ_v, Equation (7), gave the widths of the pass-bands of the filter banks in Section 3.1 from the center frequency. These widths were based on octave band decomposition, implying wide pass-bands for high frequencies and narrow pass-bands for low frequencies. If our filter bank shall have arbitrary subband decomposition, we must use alternative formulas for the pass-band widths. A wide pass-band will result in a corresponding high σ. We found the formulas

$$\sigma_u = \frac{u_{max} - u_{min}}{13.6}$$

$$\sigma_v = \frac{v_{max} - v_{min}}{13.6},$$

to be appropriate, where u and v refer to vertical and horizontal spatial frequencies, respectively, (see Figure 8) and max and min refer to upper and lower pass-band frequency, respectively.

We have one further problem to take into account. In Section 3.1 we used filter orientations in the range $0°$ to $180°$. The decomposition we have proposed here will only make it possible to specify orientations from $0°$ to $90°$. To maintain some selectiveness of angles from $90°$ to $180°$, we apply filters whose frequency responses is the sum of the frequency responses in the range $0°$ to $90°$ and the frequency response of the corresponding orthogonally oriented filter in the range $90°$ to $180°$.

The experimental results from this filtering approach, Table 3, shows that non-octave band decompositions are viable alternatives to the octave band decomposition, for some images – however not for the demanding 'Nat-16b' texture mosaic. The problem, however, remains the same for all decompositions: to achieve a good segmentation quality we need a large number of subbands, which leads to high computational complexity, as well as large memory requirements. Tab. 3

4 New filter banks for texture segmentation

The approaches presented above have either a high computational complexity, or poor classification for some textures combined with a more limited range of applications. The problem with the high computational complexity may be solved by implementing the filters in hardware – in parallel – but this implies high design and production costs. For many applications, an alternative, robust and fast, software solution is desired. We know that filtering through a bank of N filters gives rise to N feature images, each of the same size as the input image, thus we have an N-fold increase in the amount of data. To achieve correct classification we should in principle not need redundant representation. Is it possible to represent the images without redundancy, and without any critical loss in segmentation quality?

For critically sampled filter banks with perfect reconstruction, as used in image coding, see for example Husøy [23], the problem with redundancy is solved. Is it possible to achieve segmentation accuracy comparable to that of the Gabor filters, when using such filter banks? Before we go further into the experiments, we start with a short description of critically sampled filter banks.

4.1 Critically sampled filter banks – basic theory

Figure 9 shows a general *analysis* - *synthesis* filter bank. The symbol $\downarrow L$ represents *sub-sampling* by L, while the symbol $\uparrow L$ represents *up-sampling* by L. Sub-sampling by L is the process of discarding all but every L'th sample, while up-sampling by L is the process of inserting $L-1$ zeros between each sample. Fig. 9

The filter bank in Figure 9 is *critically sampled* if $L = M$, that is the sub-sampling factor is equal to the number of filters in the filter bank. A critically sampled filter bank has *perfect reconstruction* if the output of the synthesis filter bank is equal to the input to the analysis filter bank (with a possible delay). There exists a large (in fact infinite) class of filter banks with perfect reconstruction.

It is possible to implement the filtering operations of the filter banks at low sampling rate, and thereby achieve big savings in computational complexity [24]. The theory of filter banks is covered in detail in [14, 24].

We restrict our further discussion to *separable* and *tree-structured* perfect and almost perfect reconstruction filter banks. A filter bank is separable if it is possible to apply the filters in each dimension separately. A filter bank is tree-structured if it is built up as indicated in Figure 10 where each level in the tree is a two-channel filter bank. Fig. 10

We will use two types of filters, *finite impulse response* (FIR) and *infinite impulse response* (IIR). The IIR filters are based on digital *all-pass* filters, and they are given by

$$H_{LP}(z) = A_0(z^2) + z^{-1}A_1(z^2) \tag{8}$$

$$H_{HP}(z) = A_0(z^2) - z^{-1}A_1(z^2), \tag{9}$$

where

$$A_i(z) = \frac{a_i + z^{-1}}{1 + a_i z^{-1}},$$

are the first order all-pass filters. We found first-order filters to be sufficient. Thus, the IIR filters we use are attractive due to their computational simplicity [23].

4.2 Multirate texture segmentation

We have previously presented an experimental setup for multichannel filtering for texture segmentation with Gabor filters. To be able to use sub-sampled filter banks successfully, we need to make a modification to the smoothing filter in the local energy function. All other parts, except from the filter bank, remain the same.

When we decimate the signal by a factor N, a sinusoid with period M and frequency $f = 1/M$ will get the period M/N, and the frequency $N/M = Nf$. Thus, the smoothing filter designed for a given full rate signal will no further be designed for the same signal after sub-sampling. We remember that σ in Equation (3) was inversely proportional to the radial frequency f_0, therefore we use the equation

$$\sigma = \frac{\sqrt{2}}{2} \frac{1}{N f_0},$$

where N is the sub-sampling factor and f_0 is the absolute value of the center frequency of the filter bank channel.

4.3 Experimental results

To be able to study the effect of sub-sampling with respect to segmentation accuracy, we performed tests with both full rate and sub-sampled filter banks. We tested segmentation using the perfect reconstruction IIR filter banks from Husøy [23] and the nearly perfect reconstruction FIR filter banks from Johnston [25]. We performed experiments on a large number of combinations of filters, images and subband decompositions, and found the FIR filter 'f32d' and the IIR filter 'F_2_1_09' to be quite representative of the different classes of filters [26]. These filters have also been used in texture *classification* [27]. For 'F_2_1_09' the coefficient $a_0 = 0.66$, while a_1 may be zero or one, depending on the implementation, See Johnston [25] for the coefficients for 'f32d'.

Our experiments reveal that the octave band decomposition is approximately equal to the non-octave band decomposition, structure C in Figure 8, in terms of performance, see Table 4. Tab. 4

The results in Table 4 show that perfect reconstruction filters are suited to texture segmentation, when no sub-sampling of the channel filters is applied (full rate). The results we get are approximately the same as those we got with the Gabor filter. But by using full rate filters we don't achieve the desired savings in computational complexity. Is it possible to use critically sampled filter banks and achieve good segmentation? Table 5 and Figures 11, 12 and 13 show the results from our experiments. Tab. 5

Fig. 11

We see from Table 4 and 5 and Figure 11 and 12 that the segmentation Fig. 12 accuracies in the sub-sampled case are a somewhat degraded relative to the results Fig. 13 in the full rate case, nevertheless we obtain high quality segmentation even with sub-sampled perfect reconstruction filters. Remember that the computational savings are tremendous, for 'Nat-16b', for instance, we had a feature set of five megabytes in Section 3.1, now we have a feature set of only a quarter megabyte. This has large implications on the computational complexity and the memory requirements for the segmentation system.

We see that the segmentation based on critical sampling has a stair-case effect near the edges. Further experiments show, as expected, that the stair-case effect is reduced if we use a lower sub-sampling rate, but at a higher computational cost. With a sampling rate of four times the critical sampling for the texture 'Nat-5b' with the filter 'F_2_1_09' we got 97.1% correct classification and drastically reduced stair-case effect, see Figure 14. Fig. 14

Segmentation based on outputs from sub-sampled filter banks show promising results, when the filter banks have the perfect reconstruction property. However, when we are segmenting images, we do not need the perfect reconstruction property – it is only needed in image coding. What if we sub-sample filter banks without the perfect reconstruction property? To examine this idea, we performed tests on sub-sampled Gabor filters. These tests show that it is not possible to sample the Gabor filter "critically" without severely reducing the segmentation quality – for 'Nat-16b' and with structure C we only got 79.0% correct classification, or 12.8% different from the critically sampled 'F_2_1_09' filter. This, however, does not, of course, prove that non-perfect reconstruction filters yielding good segmentation doesn't exist.

5 Summary and conclusions

We have evaluated a large class of filters for multichannel filtering for texture segmentation and compared them against some approaches using the Gabor filter. It was shown that the Gabor filter is far from the only acceptable filter choice. Our experiments show that several filter banks known from image subband coding may provide results that are comparable to those of the Gabor filter. We have further shown that other subband decompositions than the octave band decomposition may be viable alternatives.

We have also shown that it is possible to use critically sampled perfect reconstruction filter banks at the cost of only a modest degradation in segmentation quality. In this way, tremendous savings in computational complexity are realized.

Note

All the test images are available via anonymous FTP on internet site `mom.spie.org` in directory `???`.

References

[1] F. Farrokhnia, *Multi-channel filtering techniques for texture segmentation and surface quality inspection.* PhD thesis, Michigan State University, 1990.

[2] F. Farrokhnia and A. K. Jain, "A multichannel filtering approach to texture segmentation," in *Proc. Computer Vision and Pattern Recognition*, pp. 364–370, IEEE Comp. Soc., 1991.

[3] A. K. Jain and F. Farrokhnia, "Unsupervised texture segmentation using Gabor filters," *Pattern Recognition*, vol. 24, no. 12, pp. 1167–1186, 1991.

[4] A. C. Bovik, "Properties of multichannel texture analysis filters," in *Proc. Int. Conf. Acoust. Speech, Signal Proc.*, (Albuquerque, NM), pp. 2133–2136, IEEE, 1990.

[5] M. R. Turner, "Texture discrimination by Gabor functions," *Biological Cybernetics*, vol. 55, pp. 71–82, 1986.

[6] A. Perry and D. G. Lowe, "Segmentation of textured images," in *Proc. Computer Vision and Pattern Recognition*, pp. 319–325, IEEE Comp. Soc., 1989.

[7] T. N. Tan and A. G. Constantinides, "Texture analysis based on a human visual model," in *Proc. Int. Conf. Acoust. Speech, Signal Proc.*, (Alberquerque, NM), pp. 2137–2140, IEEE, 1990.

[8] T. Chang and C.-C. J. Kuo, "Texture analysis and classification with tree-structured wavelet transform," *IEEE Trans. Image Processing*, vol. 2, no. 4, pp. 429–441, 1993.

[9] M. Clark and A. C. Bovik, "Experiments in segmenting texton patterns using localized spatial filters," *Pattern Recognition*, vol. 22, no. 6, pp. 707–717, 1989.

[10] J. M. Coggins and A. K. Jain, "A spatial filtering approach to texture analysis," *Pattern recognition letters*, vol. 3, no. 3, pp. 195–203, 1985.

[11] I. Ng, T. Tan, and J. Kittler, "On local linear transform and Gabor filter representation of texture," in *Proc. Int. Conf. on Patt. Rec.*, pp. 627–631, Int. Assoc. for Patt. Rec., 1992.

[12] D. Gabor, "Theory of communication," *J. Inst Elect. Engr.*, vol. 93, pp. 429–457, 1946.

[13] J. G. Daugman, "Uncertainty relation for resolution in space, spatial-frequency, and orientation optimized by two-dimensional visual cortical filters," *Journal of Optical Society of America*, vol. 2, no. 7, pp. 1160–1169, 1985.

[14] P. P. Vaidyanathan, "Quadrature mirror filter banks, M-band extensions and perfect-reconstruction techniques," *IEEE ASSP Magazine*, vol. 4, pp. 4–20, July 1987.

[15] S. G. Mallat, "Multifrequency channel decomposition of images and wavelet models," *IEEE Trans. Acoust., Speech, Signal Processing*, vol. 37, pp. 2091–2110, Dec. 1989.

[16] F. W. Campbell and J. G. Robson, "Application of fourier analysis to the visibility of gratings," *J. Physiology*, vol. 197, pp. 551–566, 1968.

[17] D. F. Dunn, W. E. Higgins, and J. Wakeley, "Determining Gabor-filter parameters for texture segmentation," in *Intelligent robots and computer vision XI*, vol. 1826, pp. 51–63, 1992.

[18] T. Kohonen, "The self-organizing map," *Proc. IEEE*, vol. 78, pp. 1464 – 1480, Sept. 1990.

[19] T. Kohonen, J. Kangas, J. Laakonen, and K. Torkkola, "LVQ-PAK: The Learning Vector Quantization program package, version 2.1." Internet FTP, 1992.

[20] P. Brodatz, *Textures: A photographic album for artists and designers.* NY: Dover, 1966.

[21] D. F. Dunn and W. E. Higgins, "Optimal Gabor-filter design for texture segmentation," in *Proc. Int. Conf. Acoust. Speech, Signal Proc.*, (Minneapolis, MN), IEEE, 1993.

[22] D. F. Dunn, W. E. Higgins, and J. Wakeley, "Texture segmentation using 2-D Gabor elementary functions," *IEEE Trans. Pattern Analysis and Machine Intelligence*, vol. 22, pp. 130–149, Feb. 1994.

[23] J. H. Husøy, "Low complexity subband coding of still images and video," *Optical Engineering*, vol. 30, pp. 904–911, July 1991.

[24] A. N. Akansu and R. A. Haddad, *Multiresolution Signal Decomposition.* San Diego: Academic Press, 1992.

[25] J. D. Johnston, "A filter family designed for use in quadrature mirror filter banks," in *Proc. Int. Conf. Acoust. Speech, Signal Proc.*, (Denver, CO), pp. 291–294, IEEE, 1980.

[26] T. Randen, "Flerkanal filtrering for tekstursegmentering," Master's thesis, Rogaland University Center, 1993 (in Norwegian).

[27] J. H. Husøy, T. Randen, and T. O. Gulsrud, "Image texture classification with digital filter banks and transforms," in *Proc. SPIE International symposium on optical instrumentation and applied science: Applications of Digital Image Processing XVI*, (San Diego), pp. 260 – 271, July 1993.

Texture mosaic	Accuracy
‘D17-D55’	98.6%
‘Nat-5b’	97.5%
‘Nat-16b’	93.4%

Table 1: Experimental results from the fixed filter structure even symmetric Gabor filter.

Texture mosaic	Accuracy
‘D17-D55’	96.4%
‘Nat-5b’	97.0%

Table 2: Experimental results from the optimal parameters method.

Structure	‘D17-D55’	‘Nat-5b’	‘Nat-16b’
A	98.1%	96.2%	79.8%
B	98.2%	95.3%	94.1%
C	98.1%	95.6%	86.6%

Table 3: Classification with the Gabor filter with various subband decompositions.

Image	'Nat-5b'		'Nat-16b'	
Structure	'F_2_1_09'	'f32d'	'F_2_1_09'	'f32d'
A	97.0%	97.1%	89.5%	89.3%
B	96.0%	95.7%	94.1%	93.5%
C	97.2%	97.2%	92.8%	92.4%

Table 4: Full rate segmentation with various subband decompositions and filters 'F_2_1_09' and 'f32d'.

Filter	'D17-D55'	'Nat-5b'	'Nat-16b'
'F_2_1_09'	96.4%	93.3%	90.4%
'f32d'	96.8%	93.7%	91.7%

Table 5: Segmentation from critically sampled filters with filter structure C.

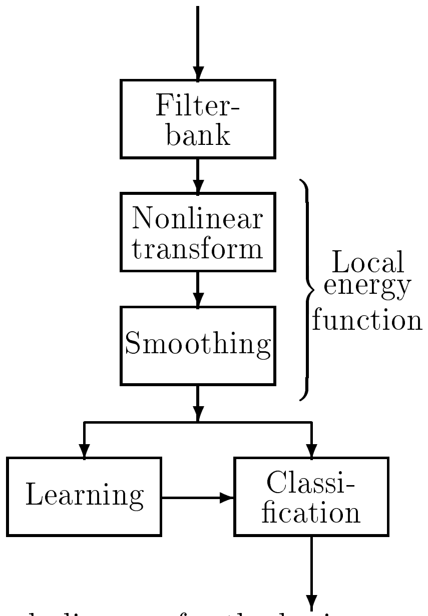

Figure 1: Block diagram for the basic experimental setup

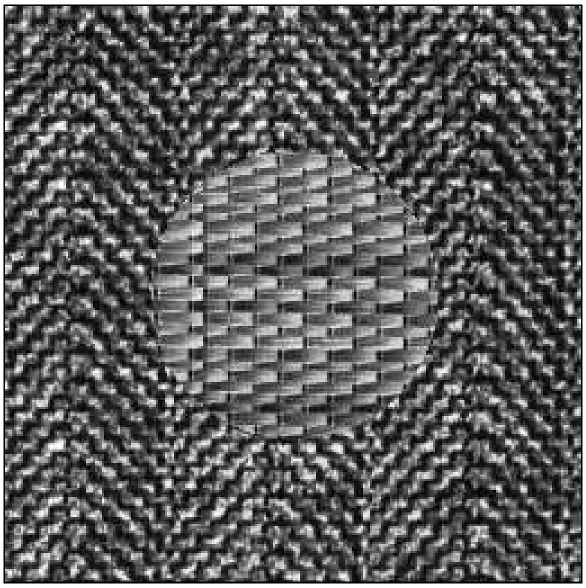

Figure 2: The 256×256 'D17-D55' texture mosaic, with the textures 'D17' and 'D55'.

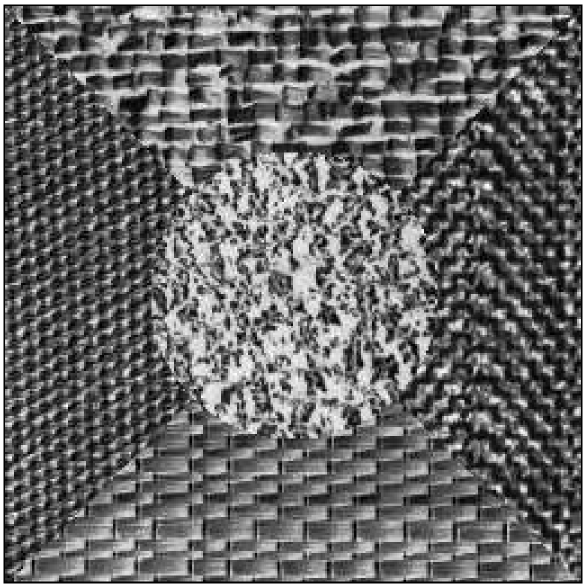

Figure 3: The 256×256 'Nat-5b' texture mosaic, with the textures 'D77', 'D55', 'D84', 'D17' and 'D24'.

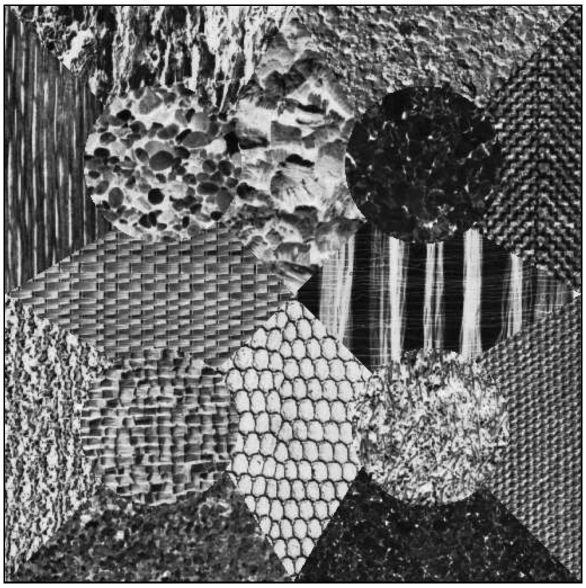

Figure 4: The 512×512 'Nat-16b' texture mosaic, with the textures 'D29', 'D12', 'D17', 'D55', 'D32', 'D5', 'D84', 'D68', 'D77', 'D24', 'D9 ', 'D4', 'D3', 'D33', 'D51' and 'D54'.

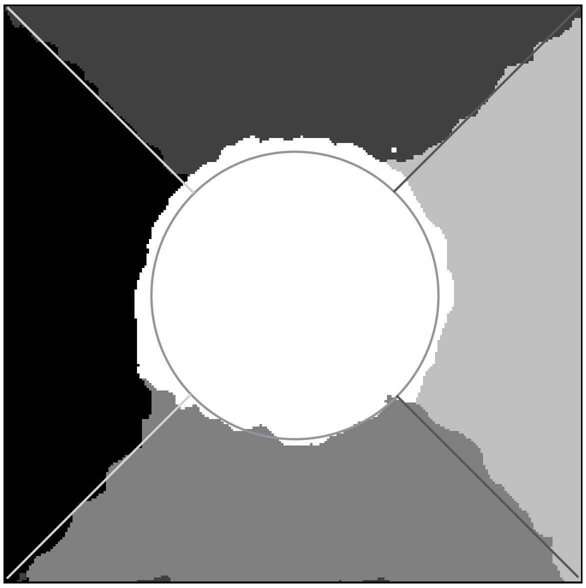

Figure 5: Segmentation results from the fixed filter structure even symmetric Gabor filter for the texture mosaic 'Nat-5b'.

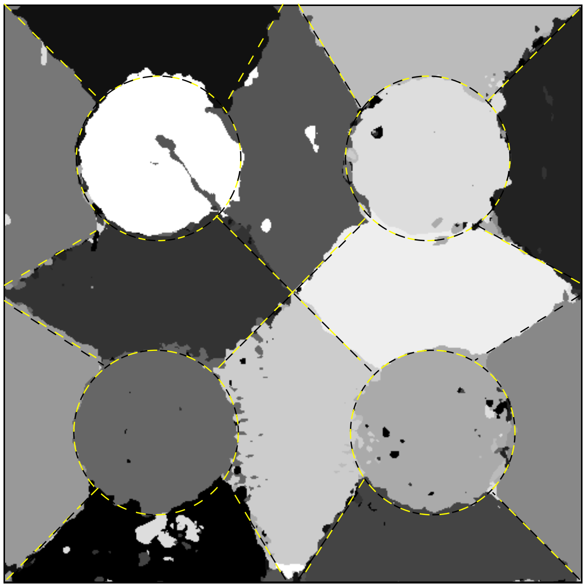

Figure 6: Segmentation results from the fixed filter structure even symmetric Gabor filter for the texture mosaic 'Nat-16b'.

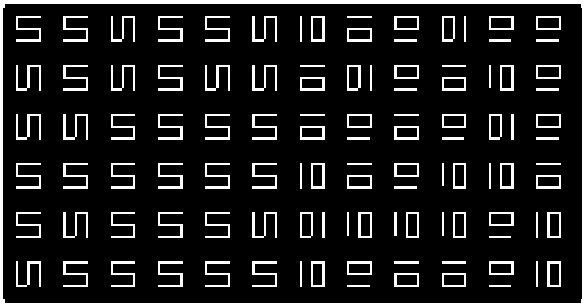

Figure 7: The texture mosaic 'S-IO'

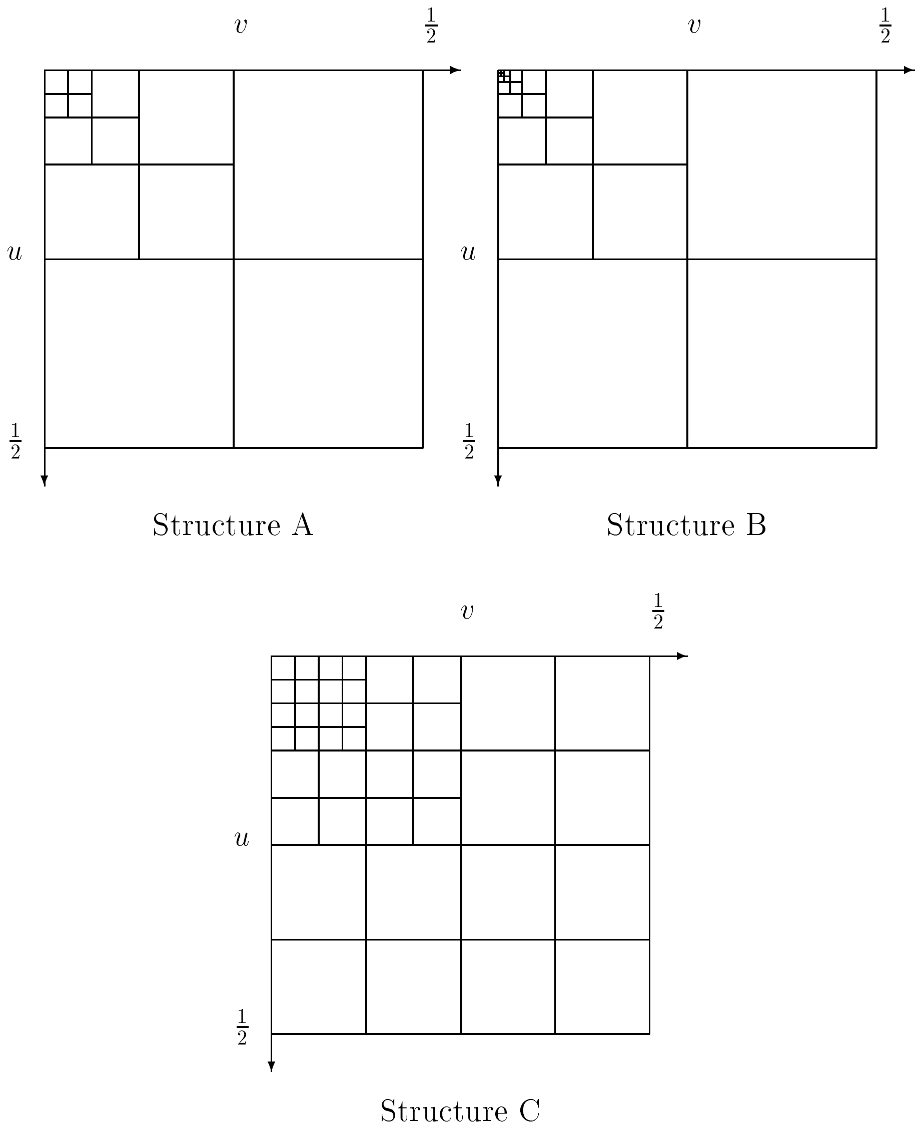

Figure 8: Subband decompositions. Structures A and B are octave band decompositions, where A has four and B has seven levels.

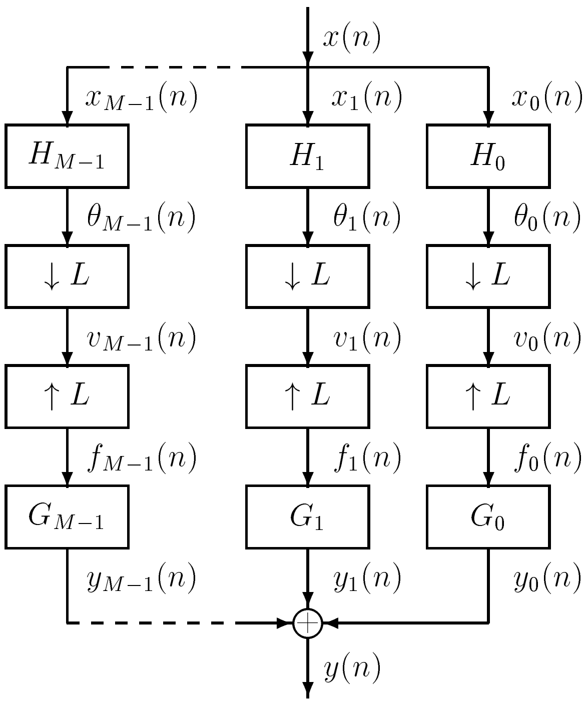

Figure 9: General analysis-synthesis filter bank.

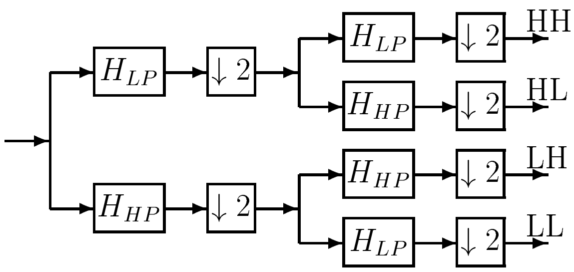

Figure 10: Tree-structured filter bank

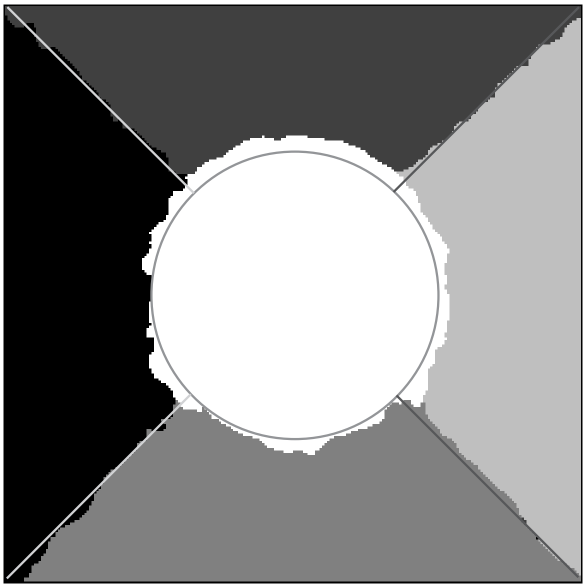

(a)

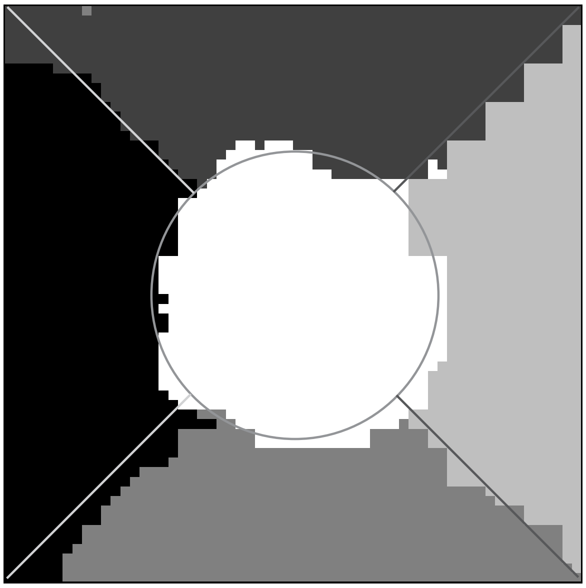

(b)

Figure 11: Segmentation results from (a) full rate 'F_2_1_06', (b) critically sampled 'F_2_1_06', (c) full rate 'f32d' and (d) critically sampled 'f32d' with the texture mosaic 'Nat-5b'.

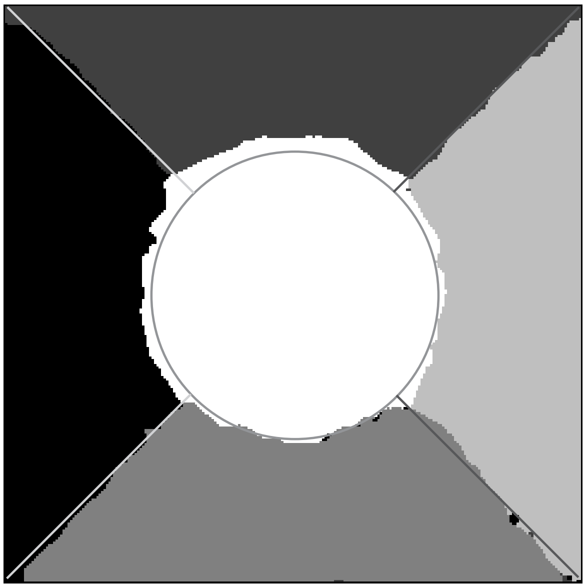

(a)

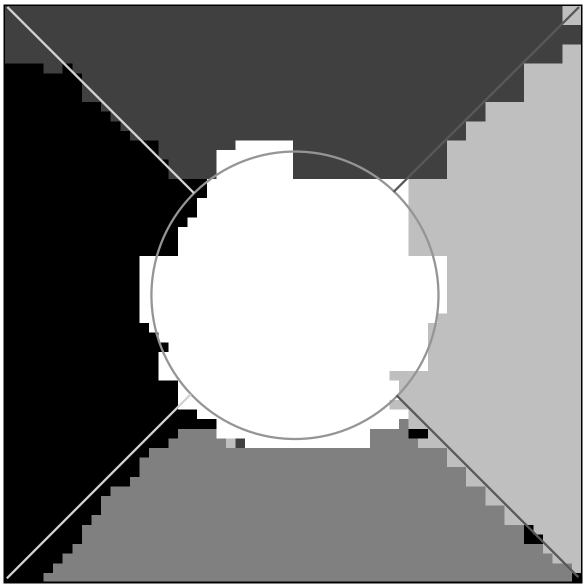

(b)

Figure 12: Segmentation results from (a) full rate 'f32d' and (b) critically sampled 'f32d' with the texture mosaic 'Nat-5b'.

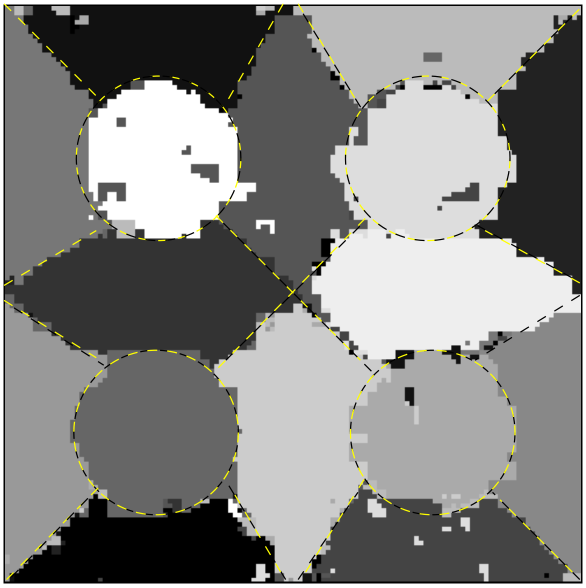

(a)

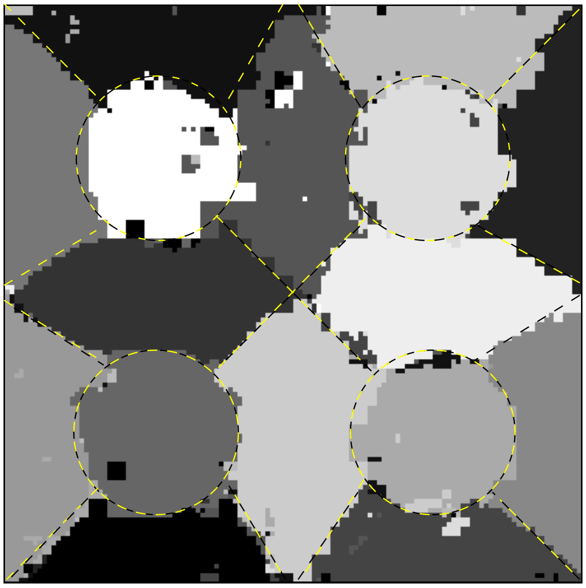

(b)

Figure 13: Segmentation results from (a) critically sampled 'F_2_1_06', (b) critically sampled 'f32d' with the texture mosaic 'Nat-16b'.

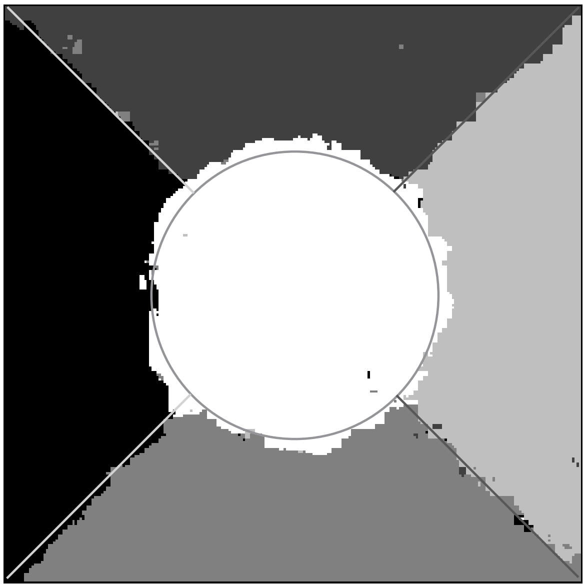

Figure 14: Segmentation result from four times critical sampling with filter structure C, filter 'F_2_1_09' and texture 'Nat-5b'.

Trygve Randen was born in Egersund, Norway in 1969. He received his B.Eng. and M.Sc. in 1991 and 1993 respectively, both from the Electrical and Computer Engineering Department at Rogaland University Center.
He is currently a research fellow and Ph.D. student at Rogaland University Center. The scheduled conclusion of his Ph.D. studies is June 1997. His main research interest is image processing with the emphasis on pattern recognition, using multi-rate signal processing, filter banks, wavelets, transforms and stochastic modelling.
Mr. Randen is a member of IEEE, SPIE, the Norwegian Society for Image Processing and Pattern Recognition (NOBIM) and the Norwegian Society for Signal Processing (NORSIG).

John Håkon Husøy was born in Toronto, Canada, in 1956. He received his M.Sc. and Ph.D. in Electrical Engineering in 1981 and 1991, respectively, from the Norwegian Institute of Technology, University of Trondheim, Norway.
>From 1982 to 1986 he worked for the Canadian Department of Transportation, Ottawa, Ontario, and subsequently for Northern Telecom, Ottawa. The following two years were spent at the Chr. Michelsen Institute, Bergen, Norway. >From 1988 to 1992 he was with the Department of Electrical and Computer Engineering at the Norwegian Institute of Technology.
In 1992 Dr. Husøy was appointed professor of Electrical and Computer Engineering at Rogaland University Center. His research interests include image compression, digital filtering, bioelectrical signal processing, adaptive algorithms and image analysis.
Dr. Husøy is a member of IEEE, EURASIP, NOBIM and NORSIG.